

Modulation of Double Zwitterionic Block Copolymer Aggregates by Zwitterion-Specific Interactions

Akane Shimizu,[§] Emi Hifumi,[‡] Ken Kojio,^{//} Atsushi Takahara,[#] Yuji Higaki^{†}*

[§]Graduate School of Engineering, Oita University, 700 Dannoharu, Oita, 870-1192, Japan

[‡]Research Promotion Institute, Oita University, 700 Dannoharu, Oita, 870-1192, Japan

^{//}Institute for Materials Chemistry and Engineering, Kyushu University, 744 Motooka, Nishi-ku,
Fukuoka 819-0395, Japan

[#]Research Center for Negative Emission Technology, Kyushu University, 744 Motooka, Nishi-
ku, Fukuoka 819-0395, Japan

[†]Department of Integrated Science and Technology, Faculty of Science and Technology, Oita
University, 700 Dannoharu, Oita, 870-1192, Japan

ABSTRACT

Transformable double hydrophilic block copolymer assemblies are valid as a bio-compatible smart macromolecular system. The molecular mechanisms in the spontaneous assembly of double zwitterionic diblock copolymers composed of a poly(carboxybetaine methacrylate) (PCB2) and a poly(sulfobetaine methacrylate) (PSB4) chains (PCB2-*b*-PSB4) were investigated by the modulation of the aggregates in response to non-detergent zwitterions. The PCB2-*b*-PSB4 diblock copolymers with a high degree of polymerization PSB4 block produced aggregates in salt-free water through “zwitterion-specific” interactions. The PCB2-*b*-PSB4 aggregates were dissociated by the addition of non-detergent sulfobetaine (SB4) and carboxybetaine (CB2) molecules, while the aggregates showed different aggregation modulation processes for SB4 and CB2. Zwitterions with different charged groups from SB4 and CB2, glycine and taurine, hardly disrupted the PCB2-*b*-PSB4 aggregates. The PCB2₄₃-*b*-PSB4₁₅₈ aggregate modulation efficiency of SBs associated with the inter-charge hydrocarbon spacer length (CSL) rather than the symmetry with the SB in the PSB chain. These zwitterion-specific modulation behaviors were rationalized based on the nature of zwitterions including partial charge density, dipole moment, and hydrophobic interactions depending on the charged groups and CSL.

INTRODUCTION

Micellar aggregates and vesicles, which are produced by the spontaneous association of amphiphilic molecules in the solutions, are valid as a container of drugs and cosmetic ingredients with targeted transport and sustained release capability.¹ The molecular containers composed of natural and synthetic lipids often encounter problems in substance transport because of the low structural stability. Amphiphilic block copolymers have been developed as robust but upward alternatives to lipids.²⁻⁶ Spherical micelles with core-shell architecture and/or vesicles enclosed by bilayers are produced by the self-assembly of amphiphilic macromolecules in the aqueous solutions. The self-assembly is driven by the aggregation of the hydrophobic segments in aqueous environments through the hydrophobic interactions involving the entropic effects originating from the disruption of the hydrogen bonding network of water.⁷ Because of the greater synthetic diversity, various polymer micelles and vesicles modifying the stability, permeability, stimuli responsibility, and selective loading/release properties have been developed.²⁻⁶ However, the macromolecular assemblies produced by amphiphilic block copolymers involve essential limitations due to the hydrophobic domains and/or membranes. The hydrophobic domains are unsuitable for the transport of hydrophilic substances, and the hydrophobic membranes block their permeation. Meanwhile, non-amphiphilic double hydrophilic block copolymers also produce molecular assemblies driven by the interactions competing with water.⁸⁻¹⁴ These macromolecular assemblies produced by double hydrophilic block copolymers are expected as hydrophilic substance permeable systems that would be valid for crosstalk through material transport.

Poly(zwitterion)s have been paid attention as outstanding bio-inert polymers alternative to poly(ethylene glycol), which has been utilized in the passivation of biomaterials.¹⁵⁻

²⁰ The outstanding biocompatibility of polyelectrolytes is often attributed to the neutral net charge and natural hydrogen bonding network of the hydrated waters. Although the zwitterionic polymers involve positive and negative charged groups, the net charge is approximately neutral because the numbers of charged groups are completely balanced. The charged groups are well hydrated due to the charge-dipole interactions, while the hydrogen bonding network structure of the local bound water is equivalent to bulk water. Thus, the interaction with charged particles including biopolymers is so weak that the non-specific adsorption is suppressed. Besides, poly(zwitterion)s exhibit unique self-assembly behavior depending on the zwitterion structure, molecular weight, and polymer concentration.¹⁹⁻²³ Polycarboxybetaines (PCB) dissolve in salt-free water, whereas polysulfobetaines (PSB) aggregate in salt-free water due to the cohesive interaction of sulfobetaine (SB) groups.¹⁹ The SB couples dissociate in aqueous electrolyte solutions due to the charge screening effect. Matsuoka and coworkers reported that block copolymers composed of PCB and PSB chains produce spherical core-shell micellar aggregates in salt-free water, while the micelles dissociate in response to temperature and salts.²⁴⁻²⁶ We showed the lyotropic microphase separation in high concentration aqueous solutions of a block copolymer composed of poly(2-[(*N*-2-methacryloyloxyethyl-*N,N*-dimethyl)ammonio]acetate) (PCB2) and poly(3-[(*N*-2-methacryloyloxyethyl-*N,N*-dimethyl)ammonio]butane-1-sulfonate) (PSB4) (PCB2-*b*-PSB4) and the polymer concentration-dependent morphology transition.²⁷ Thus, the double zwitterionic block copolymers could be regarded as a new type of double hydrophilic block copolymers that produce ordered aggregates, however, the molecular mechanisms in the phase separation have not yet been elucidated. Here, we were reminded of the question, “Why the PCB2-*b*-PSB4 diblock copolymers render phase separation in water even

though the similarity of chemical structure, both blocks are hydrophilic polymethacrylate with zwitterion pendant groups?”.

In this paper, we address the molecular mechanisms in the assembly of double zwitterionic diblock copolymers, PCB2-*b*-PSB4, by examining the modulation of the aggregates in response to zwitterions. The aggregation behavior was verified by the hydrodynamic radius of gyration (R_h) determined by dynamic light scattering (DLS) measurement. The zwitterion-specific modulation behaviors are associated with the nature of zwitterions including partial charge density, dipole moment, and hydrophobic interactions depending on the charged groups and inter-charge hydrocarbon spacer length (CSL).

EXPERIMENTAL SECTION

Materials.

2-[(*N*-2-methacryloyloxyethyl-*N,N*-dimethyl)ammonio]acetate was a kind donation from Osaka Organic Chemical Industry Ltd. (Osaka, Japan), and used without further purification. 2-(Dimethylamino)ethyl methacrylate (FUJIFILM Wako Pure Chemical Corp., 99.0%) and acetonitrile (FUJIFILM Wako Pure Chemical Corp., 99.5%) was purified by distillation in the presence of calcium hydride. The SB with CSL of 2 (SB2), 4 (SB4), and 6 (SB6), were synthesized following literature.²⁸ The carboxybetaine (CB) with CSL of 2 (CB2) was synthesized by the reaction of *N,N*-dimethyl ethyl amine and monochloroacetic acid (See Supporting Information). The chemical structures are shown in **Figure 1**. Other reagents were purchased from Sigma-Aldrich, FUJIFILM Wako Pure Chemical Corp., or Tokyo Chemical Industry Co., Ltd., and used as received. Milli-Q water (Millipore Inc., Billerica, MA) with a resistance of >18 M Ω ·cm was used for solution preparation and dialysis. PCB2-*b*-PSB4 diblock

copolymers (**Figure 1**), and PCB2 and PSB4 homopolymers were synthesized through radical addition-fragmentation chain transfer polymerization following the previous report.²⁷ Since the association of the zwitterionic polymers is sensitive to the residual salt, the product polymers were thoroughly purified through dialysis with regenerated cellulose membrane (MWCO 3500) to remove salts and monomers. The number-average molecular weight (M_n) and molecular weight distribution (M_w/M_n) were determined by gel permeation chromatography (GPC). Characterization of the synthesized PCB2 macro-CTA, PCB2-*b*-PSB4, PCB2 homopolymers, and PSB4 homopolymers is summarized in **Table 1**. The PCB2-*b*-PSB4 copolymers are identified by the degree of polymerization (DP) as the subscript numbers.

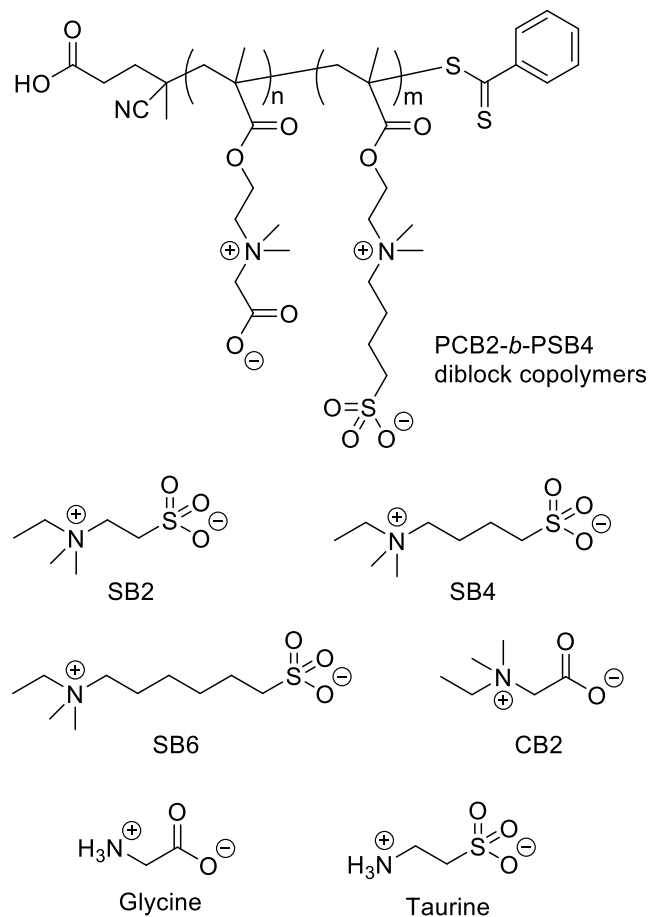


Figure 1. Chemical structure of the PCB2-*b*-PSB4 diblock copolymers and zwitterions employed in this study. The numbers in the abbreviation indicate the carbon numbers between the charged groups. The dipole moment of zwitterions with equilibrium geometry calculated by DFT calculation, SB2: 23.86, SB4: 36.27, SB6: 48.52.

Table 1. Characterization of PCB2-*b*-PSB4 diblock copolymers, and PCB2, PSB4 homopolymer

Sample ID ^a	M_n^b	M_w/M_n^b
PCB2 ₄₃ - <i>b</i> -PSB4 ₁₅₈ ^c	55800	1.08
PCB2 ₄₃ - <i>b</i> -PSB4 ₇₇ ^c	32100	1.10
PCB2 ₄₃ - <i>b</i> -PSB4 ₄₀ ^c	21100	1.11
PCB2 ₂₇	5800	1.06
PCB2 ₈₃	18000	1.14
PCB2 ₁₅₀	32400	1.10
PSB4 ₄₃	12700	1.07
PSB4 ₁₀₂	30200	1.10
PSB4 ₁₄₅	42700	1.09

^aThe subscript numbers in the sample ID indicate the degree of polymerization determined based on the M_n values. ^bDetermined by GPC measurement. ^cThe M_n and M_w/M_n of the PCB₄₃ macro-CTA were determined by GPC measurement to be 9500 and 1.11, respectively.

Measurements.

Detailed experiment conditions for ¹H-NMR and GPC are provided in the Supporting Information.

DLS measurements were performed with a Zetasizer Nano ZS (Malvern Instruments Ltd., Malvern, UK) equipped with a He-Ne laser ($\lambda = 633$ nm, 4.0 mW) and an APD detector at 25°C. The detector was preset at the scattering angle of 173°. The backscattering setup has the advantage that the effect of giant particles including dust is reduced. The freeze-dried PCB2-*b*-PSB4 was dissolved in aqueous solutions, then filtered with a hydrophilic PTFE membrane filter (ADVANTEC, HP020AN, pore size: 0.2 μ m). The sample solution was introduced in a disposable

12 mm square polystyrene cuvette (DTS0012), and the cuvette was installed in the thermostat sample holder.

The normalized intensity autocorrelation function $g^{(2)}(q, t)$, where $q = 4\pi n_D \sin\theta/\lambda$, n_D is the refractive index of water, λ is the wavelength of the incident laser (633 nm), and 2θ is the scattering angle, was obtained by a correlator. Then, the normalized electric field autocorrelation function $g^{(1)}(q, t)$ was given according to the Siegert relation:

$$g^{(2)}(q, t) = 1 + \beta |g^{(1)}(q, t)|^2 \quad (1)$$

where β is a coherence factor. For a polydisperse particle system, the $g^{(1)}(q, t)$ can be written as

$$g^{(1)}(q, t) = \int_0^\infty A(\Gamma) \exp(-\Gamma\tau) d\Gamma \quad (2)$$

where $A(\Gamma)$ is the normalized distribution of decay rates. Each autocorrelation function was analyzed by the software provided by the manufacturer. The translational diffusion coefficients D ($=\Gamma/q^2$) were calculated from the slope of the decay rate Γ versus q^2 . The hydrodynamic radius of gyration R_h was then calculated by the Stokes–Einstein equation:

$$R_h = \frac{k_B T}{6\pi\eta D} \quad (4)$$

where k_B is the Boltzmann constant, T is the absolute temperature, and η is the viscosity of solvent (water), respectively. In this article, the polymer concentration of the solutions was adjusted to 1 mg/mL in all DLS experiments, and the solution viscosity was approximated to that

of water. DLS data were shown with R_h distribution and scattering intensity normalized with the maximum of the distribution in order to clearly show the modulation of aggregate R_h distribution. DLS results are summarized in **Table 2**. The volume-normalized fraction of unimers and aggregates are shown in the brackets.

Table 2. Hydrodynamic radius of gyration of unimers and aggregates of PCB2-*b*-PSB4 diblock copolymers in the aqueous solutions

polymer	salt	salt conc. (mM)	R_h (nm) ^a	
			unimers	aggregates
PCB2 ₄₃ - <i>b</i> -PSB4 ₄₀	—	—	5.0 (99.9)	89.9 (0.1)
PCB2 ₄₃ - <i>b</i> -PSB4 ₇₇	—	—	4.6 (93.5)	26.8 (6.3)
PCB2 ₄₃ - <i>b</i> -PSB4 ₁₅₈	—	—	—	40.5
PCB2 ₄₃ - <i>b</i> -PSB4 ₁₅₈	CB2	10	—	59.2
PCB2 ₄₃ - <i>b</i> -PSB4 ₁₅₈	CB2	100	—	81.2
PCB2 ₄₃ - <i>b</i> -PSB4 ₁₅₈	CB2	1000	9.6 (98.8)	92.3 (1.1)
PCB2 ₄₃ - <i>b</i> -PSB4 ₁₅₈	SB2	10	—	37.3
PCB2 ₄₃ - <i>b</i> -PSB4 ₁₅₈	SB2	100	—	35.4
PCB2 ₄₃ - <i>b</i> -PSB4 ₁₅₈	SB2	1000	10.3 (99.3)	96.4 (0.4)
PCB2 ₄₃ - <i>b</i> -PSB4 ₁₅₈	SB4	10	—	37.2
PCB2 ₄₃ - <i>b</i> -PSB4 ₁₅₈	SB4	100	—	34.6
PCB2 ₄₃ - <i>b</i> -PSB4 ₁₅₈	SB4	1000	12.7	—
PCB2 ₄₃ - <i>b</i> -PSB4 ₁₅₈	SB6	10	—	31.8
PCB2 ₄₃ - <i>b</i> -PSB4 ₁₅₈	SB6	100	8.1	—
PCB2 ₄₃ - <i>b</i> -PSB4 ₁₅₈	SB6	1000	11.5 (96.9)	97.9 (3.1)

^aDetermined by DLS measurement at 25°C. The volume-normalized fraction was shown in the brackets.

RESULTS AND DISCUSSION

PCB2-*b*-PSB4 Assemblies in Salt-free Aqueous Solutions

The PCB2-*b*-PSB4 diblock copolymers produced aggregates in the salt-free aqueous solutions, while the DP of the PSB4 chain is required to be sufficiently high for all PCB2-*b*-PSB4 chains to be fully involved in the association (**Figure 2**). The PCB₂₄₃-*b*-PSB₄₁₅₈ formed uniform aggregates ($R_h = 40.5$ nm) with narrow polydispersity, whereas the diblock copolymer chains existed as the isolated single chain, namely “unimer”, in the case of PCB₂₄₃-*b*-PSB₄₇₇ and PCB₂₄₃-*b*-PSB₄₄₀. The PCB₂₄₃-*b*-PSB₄₇₇ partly produced aggregates with broad polydispersity, while the PCB₂₄₃-*b*-PSB₄₄₀ hardly produced aggregates. Since the scattering light intensity is proportional to the sixth power of the size of the scattering bodies, the integration of the normalized scattering intensity is not consistent with the population of the scattering objects. As shown in **Table 2**, the volume-normalized fractions of the large R_h aggregates are minor if the unimers and aggregates coexist, thus most chains exist as unimer. As proposed by Matsuoka and coworkers, the PCB-*b*-PSB diblock copolymers produce core-shell structure micelles, where the core consists of the PSB networking with the SB couples and the shell consists of water-soluble PCB.²⁴ Since the PCB chains prevent excess aggregation number, the R_h is limited to several tens of nanometers. The significant cohesive interaction force in the PSB chains is attributed to the balanced charge density in the SB groups.²⁹ Thus, the PCB-*b*-PSB spontaneously produced the micellar assemblies through “zwitterion-specific” interactions of the zwitterion pendant groups, in other words, the SBs efficiently interact with SB rather than CB in the system.

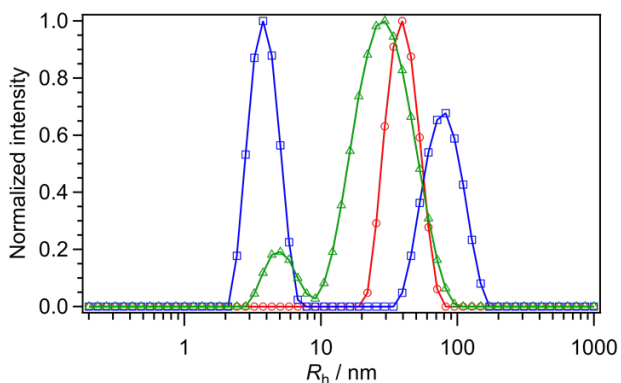


Figure 2. R_h distributions of (a) PCB₂₄₃-*b*-PSB₄₄₀ (blue squares), (b) PCB₂₄₃-*b*-PSB₄₇₇ (green triangles), and (c) PCB₂₄₃-*b*-PSB₄₁₅₈ (red circles) aggregates in salt-free water at 25°C. The lines are given for visual clarity.

The impact of molecular weight on the PCB2-*b*-PSB4 assembly was verified by the aggregation behavior of PSB4 and PCB2 homopolymers. The PSB4 homopolymers with a high DP of over 102 produced large aggregates in salt-free water, whereas those with a low DP of 43 hardly produce aggregates (**Figure 3(a)**). The high DP PSB4 solutions were opaque, while the low DP PSB4 solutions were transparent. Interestingly, the PCB2 homopolymers with a low DP of 27 produced aggregates in salt-free water ($R_h = 45.2$ nm), whereas those with high DP of over 83 hardly produce aggregates (**Figure 3(b)**). These contrasting results could be attributed to the difference in aggregation mechanisms in the PSB4 and PCB2. The SB4 zwitterion involves a long hydrocarbon spacer between the quaternary ammonium cation and sulfonate anion. The charge separation induces the increase of the dipole moment because the dipole moment p is the product of the charge q and charge distance d ($p = qd$), while the long hydrocarbon chain brings hydrophobicity to the zwitterions. Thus, the SB4 is hydrophilic due to the large charge-dipole and dipole-dipole interactions with water, while the aggregation is promoted through the hydrophobic

and dipolar interactions. It should be noted that hydrocarbon charge spacer is rarely all-trans rather looped conformation to approach the charged groups.^{30,31} Meanwhile, the CB2 zwitterion involves a short hydrocarbon spacer between the quaternary ammonium cation and carboxylate anion. The charge proximity reduces the effective partial charge of the CB2 due to the charge interplay, while the short hydrocarbon induces a weak impact on the hydrophobic interactions. Thus, the CB2 is poorly hydrophilic due to the weak charge-dipole and dipole-dipole interactions, whereas the aggregation is not promoted due to the poor hydrophobic interactions. The electrostatic potential and dipole moment of the zwitterions were calculated with DFT calculations (**Table S1**). The weak dipole moment and poor energy of CB2 in contrast with the SB4 were verified through the calculation.

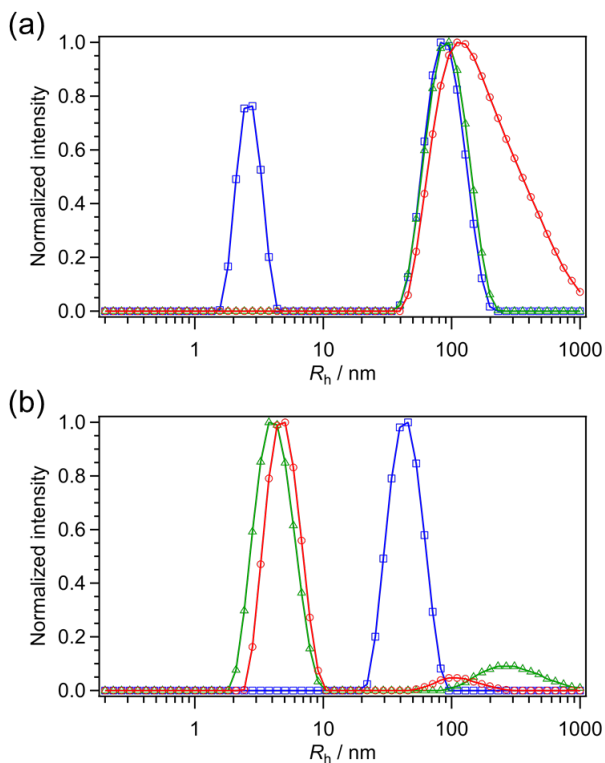


Figure 3. R_h distributions of aggregates produced by assembly of (a) PSB4 [DP: 43 (blue squares), 102 (green triangles), 145 (red circles) and (b) PCB2 [DP: 27 (blue squares), 83 (green triangles), 150 (red circles)] homopolymers in salt-free water at 25°C. The lines are given for visual clarity.

The SB4 zwitterion requires enough association frequency to produce the inter-chain networking, thus the aggregation is promoted with increasing the molecular weight and polymer concentration. The short PSB4 chains exist as unimer because of the small number of SB4 couples and the hydrophilicity of the non-coupled SB4 groups. Meanwhile, the short PCB2 chains aggregate through hydrophobic interactions of the hydrocarbon main chain rather than CB2 coupling because the CB2 zwitterions in the repeating units are not sufficiently hydrophilic due to the interplay of close charges. The non-electrostatic association of the PCB2 was verified by the ionic strength dependence of the PCB2 aggregates (**Figure S2**). The R_h and the distribution of the

short PCB2 aggregates hardly depended on the NaCl concentration of the solutions indicating that the aggregates are assembled by the non-electrostatic interactions.

Matsuoka and coworkers reported systematic studies for the aggregation of double zwitterionic diblock copolymers composed of PCB2 and PSB with CSL of 3 (the carbon number between the charges is 3; PSB3) in aqueous solutions.²⁴⁻²⁶ The PCB2-*b*-PSB3 block copolymers produce spherical core-shell micelles as shown in the shape factor (R_g/R_h) values. The micellar assemblies dissociate by thermal activation because of the dissociation of the PSB3 chains which show upper critical solution temperature. Furthermore, the SB couple dissociation is promoted by the interaction with ions, and the efficiency depends on the ion species.²²⁻²⁵ Although the PCB2-*b*-PSB4 diblock copolymers studied in this study consists of a PSB chain with longer CSL (the carbon number between the charges is 4), the aggregation behavior, impact of ions, and ion-specificity in the dissociation of the micellar aggregates were almost consistent with PCB2-*b*-PSB3 (**Figure S3, S4**). It should be noted that the temperature responsibility is diminished because of the enhanced association efficiency of PSB4, whereas the ion-responsibility was promoted due to the charge separation with long hydrocarbon.²² The PCB2-*b*-PSB4 aggregates hardly changed the R_h by thermal activation at around 70°C, thus the sulfobetaine couples in the PSB4 aggregates maintain their binding (**Figure S5**). Besides, the association behavior relates with the polymer concentration,²² but the impact of polymer concentration has not been discussed in this paper due to the constraints of DLS measurement.

Zwitterion-Specific Modulation of PCB2-*b*-PSB4 Assemblies

Impact of Charged Groups in the Zwitterions

To address the zwitterion-specific interactions in the PCB2-*b*-PSB4 assemblies, modulation of the aggregates by the addition of zwitterions was investigated. First, the impact of a non-detergent SB compound with CSL of 4 (SB4), which is the symmetric zwitterion to the PSB4 pendant zwitterion, to the modulation of the PCB2-*b*-PSB4 aggregates was studied. Since the PCB2₄₃-*b*-PSB4₁₅₈ produces the most uniform aggregates in the series of PCB2-*b*-PSB4 used in this study, the experiments described below were performed using the PCB2₄₃-*b*-PSB4₁₅₈. The PCB2₄₃-*b*-PSB4₁₅₈ aggregates maintained the form at the low SB4 concentrations of 10 mM and 100 mM, while the aggregate completely dissociated in the high SB4 concentration of the 1 M solution (**Figure 4(a)**).

Second, the impact of a non-detergent CB compound with CSL of 2 (CB2), which is the symmetric zwitterion to the PCB2 pendant zwitterion, to the modulation of the PCB2-*b*-PSB4 aggregates was verified. The CB2 enlarged the aggregate size with increasing the CB2 concentration, reaching $R_h = 59.2$ nm at 10 mM and $R_h = 81.2$ nm at 100 mM, while the aggregates dissociated in the extremely high CB2 concentration of the 1 M solution (**Figure 4(b)**).

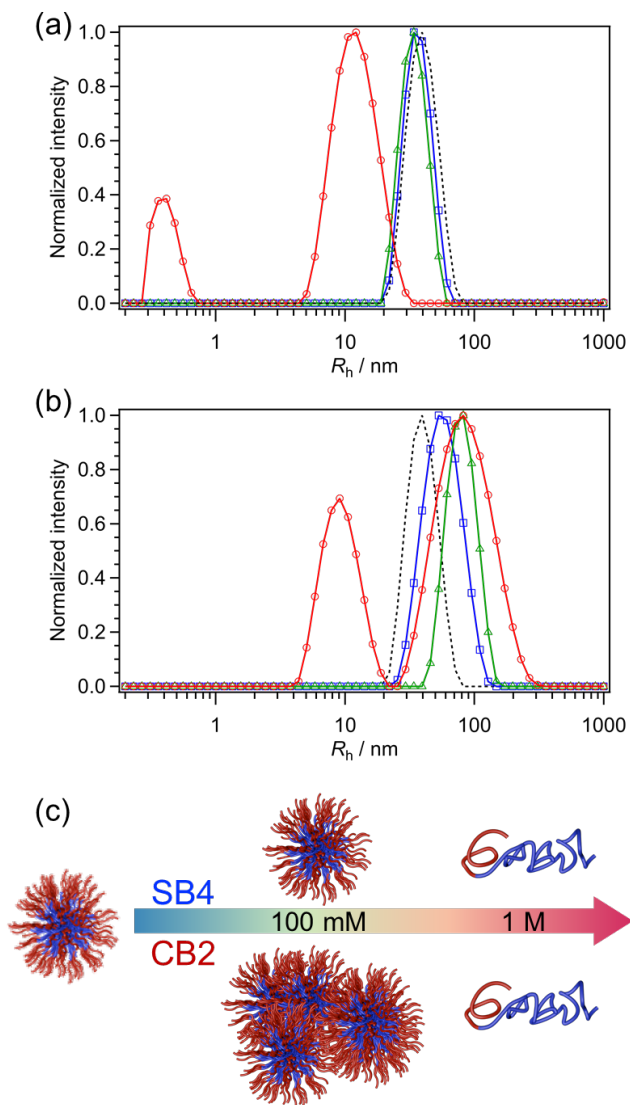


Figure 4. R_h distributions of $\text{PCB}_{243}\text{-}b\text{-PSB}_{4158}$ aggregates in (a) SB4 and (b) CB2 solutions at 25°C. The concentration of the non-detergent zwitterions was adjusted to 10 mM (blue squares), 100 mM (green triangles), and 1 M (red circles). The data for the $\text{PCB}_{243}\text{-}b\text{-PSB}_{4158}$ aggregates in salt-free water is shown with black dotted lines. The lines are given for visual clarity. (c) Schematic representation of the $\text{PCB}_{243}\text{-}b\text{-PSB}_{4158}$ aggregation behavior in response with SB4 and CB2.

The zwitterion-specific modulation of aggregates is ascribed by the aggregation state of the two kinds of zwitterions, SB4 and CB2 groups, in the PCB₂₄₃-*b*-PSB₄₁₅₈ aggregates. The SB4 molecules introduced in the PCB₂₄₃-*b*-PSB₄₁₅₈ solutions would hardly penetrate inside the micelles at low SB4 concentrations because of the osmotic demand. Besides, the SB4 molecules hardly interact with the CB2 groups in the shell. Thus, the aggregate size hardly changes through the addition of low concentration SB4. However, in the high SB4 concentration solutions, the SB4 penetrates the core, then swaps the SB couples leading to the dissociation of PCB₂₄₃-*b*-PSB₄₁₅₈ chains. On the other hand, the CB2 molecules induce the aggregation of the micelles. The CB2 would bind with PCB2 shell chains to promote aggregation through hydrophobic interactions. Contrary to our expectation based on zwitterion-specific interactions, the PCB₂₄₃-*b*-PSB₄₁₅₈ aggregates dissociated in the 1 M CB2 solution. This result implies that the SB4 couples dissociate in the presence of a large amount of CB2. We assume that the CB2 molecules are introduced inside micelles overcoming the osmotic barrier at high CB2 concentration, then induce charge screening for the SB4 groups similar to monatomic ions such as sodium cation and chloride anion. Although the partial charges are diminished through the charge approach, the CB2 could behave as a “dipolar ion”. Thus, the CB2 is capable to induce the SB4 couple dissociation through charge binding.

Other types of zwitterions with different pairs of charged groups were examined. Glycine is one of the most abundant amino acids in living bodies, and it exists as a zwitterion with a carboxylate anion and a protonated amine cation in physiological conditions. Taurine is a zwitterion widely distributed in animal tissues and is composed of a sulfonate anion and a protonated amine cation. In contrast to SB4 and CB2, the PCB₂₄₃-*b*-PSB₄₁₅₈ aggregates hardly changed the form in the presence of glycine and taurine even in the extremely high concentration 1 M solutions (**Figure S6, S7**). The zwitterions are likely to get in the micelle, however, hardly

cause the modulation of aggregates probably because the charge screening efficiencies of glycine and taurine are poor than SB and CB due to the asymmetric charged groups in the zwitterions. Thus, the symmetry of charged groups is critically associated with the modulation efficiency of the double zwitterionic PCB₂₄₃-*b*-PSB₄₁₅₈ aggregates.

Impact of Charge Distance in the Sulfobetaines

The impact of charge separation in the zwitterion to the PCB₂-*b*-PSB₄ aggregate modulation efficiency was verified using three kinds of SBs with various carbon numbers of the inter-charge methylene spacer, SB₂, SB₄, and SB₆ (**Figure 1**). The SBs were introduced into the PCB₂₄₃-*b*-PSB₄₁₅₈ solutions, and the R_h of the aggregates were determined by DLS measurement (**Figure 4(a)**, **Figure 5**).

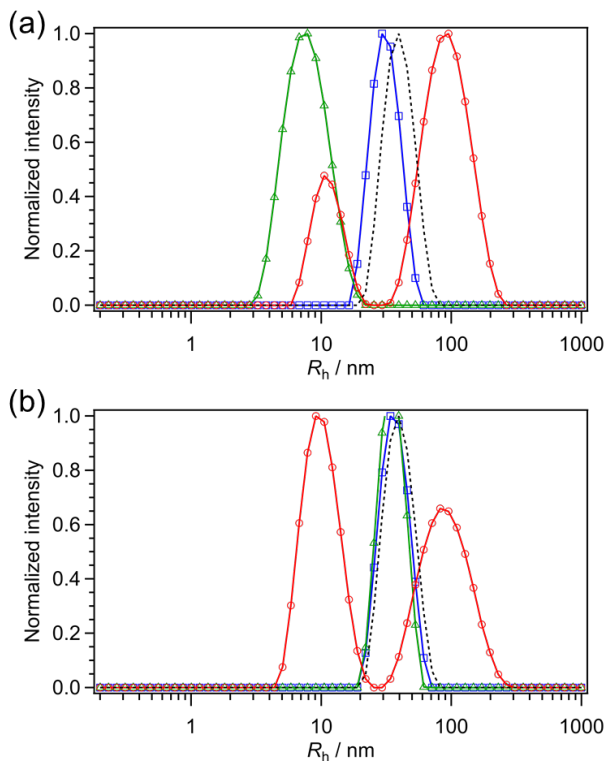


Figure 5. R_h distributions of PCB₂₄₃-*b*-PSB₄₁₅₈ in (a) SB6 and (b) SB2 solutions. The concentration of the non-detergent zwitterions was adjusted to 10 mM (blue squares), 100 mM (green triangles), and 1 M (red circles). The data for the PCB₂₄₃-*b*-PSB₄₁₅₈ aggregates in salt-free water is shown with black dotted lines. The lines are given for visual clarity.

All SBs showed induction of the PCB₂₄₃-*b*-PSB₄₁₅₈ aggregate dissociation, while the impact got significant with increasing the SB concentration. Interestingly, the SB6 showed the most significant impact as shown in the lowest induction concentration. Although the PCB₂₄₃-*b*-PSB₄₁₅₈ aggregates hardly transform at 100 mM SB4 concentration, the SB6 caused the dissociation of the aggregate even at the 100 mM SB6 concentration. Meanwhile, the SB2 showed poor impact on the PCB₂₄₃-*b*-PSB₄₁₅₈ aggregate dissociation, as shown that a small number of aggregates remained even at 1 M SB2 concentration. Thus, the PCB₂₄₃-*b*-PSB₄₁₅₈ aggregate

modulation efficiency of SBs associates with the CSL rather than the symmetry of the CSL, where the longer the CSL, the higher the modulation efficiency. Since the electrostatic and dipolar interactions are augmented by separating the charges, the SB6 shows significant swapping efficiency and charge screening effect than the SB4. In addition, the SB with long CSL, which can adopt a variety of conformations, including looped and extended, would exhibit high shielding efficiency in contrast to the SBs with short CSL, in which the conformation is relatively fixed. In the same scenario, the poor modulation efficiency of SB2 is rationalized.

Besides, the SB6 induced the aggregation of PCB₂₄₃-*b*-PSB₄₁₅₈ chains at an extremely high concentration of 1M. This re-entrant behavior could be attributed to the hydrophobicity of coupled SB pendant groups. The SB6 binding results in the dissociation of inter-chain SB4 couples leading to the dissociation of the PCB₂₄₃-*b*-PSB₄₁₅₈ aggregates. Meanwhile, the SB4 pendant groups coupled with SB6 diminish the hydrophilicity due to the charge interplay and the long hydrocarbon spacer, causing the aggregation by the hydrophobic interactions. In order to illustrate the discussion clearly, the CSL-specific modulations of PCB₂-*b*-PSB₄ aggregates based on the above discussion are depicted in **Figure 6**.

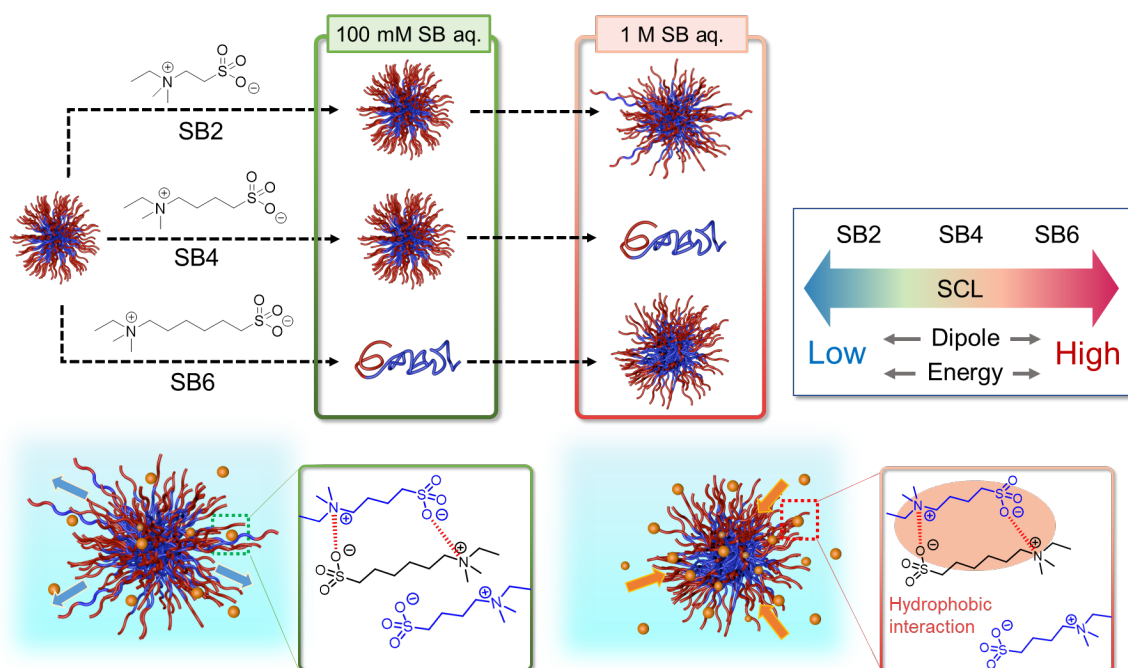


Figure 6. Schematic representation of $\text{PCB}_{243}\text{-}b\text{-PSB}_{4158}$ aggregate modulation depending on the CSL-specific zwitterion interactions.

CONCLUSION

The zwitterion-specific interactions in the $\text{PCB}_2\text{-}b\text{-PSB}_4$ double zwitterionic diblock copolymers were addressed by the modulation of the aggregates in response to various zwitterions. The $\text{PCB}_2\text{-}b\text{-PSB}_4$ diblock copolymers produce core-shell spherical micelles with PSB4 core and PCB2 shell in salt-free water through the zwitterion-specific interactions of the SB4 and CB2 groups. The PSB4 aggregates through inter-chain networking with SB4 binding, thus requiring high DP to produce the aggregates. Meanwhile, the PCB2 aggregates through hydrophobic interaction, and the aggregation is limited to the low DP case. The $\text{PCB}_{243}\text{-}b\text{-PSB}_{4158}$ aggregates are dissociated by the addition of SB4 and CB2 molecules, whereas the aggregates behaved in different aggregation modulation processes for SB4 and CB2. The $\text{PCB}_{243}\text{-}b\text{-PSB}_{4158}$ aggregate

modulation efficiency of SBs is associated with the CSL rather than the symmetry of the CSL. The peculiar zwitterion-specific interactions are rationalized based on the nature of zwitterions including partial charge density, dipole moment, and hydrophobic interactions depending on the charged groups and CSL. The dynamic double hydrophilic polymer micelles transformable with zwitterion-specific interactions are valid for the design of bio-compatible smart molecular systems for medical applications.

ASSOCIATED CONTENT

Supporting Information. The Supporting Information is available free of charge on the ACS Publications website. Measurement conditions; Synthesis of non-detergent zwitterions; Dipole moment and energy of zwitterions determined by DFT calculations; Impact of NaCl concentration to the PCB₂₇ aggregates; Impact of NaCl concentration and ion-specific modulation of the PCB₄₃-*b*-PSB₁₅₈ aggregates; Impact of temperature to the PCB₄₃-*b*-PSB₁₅₈ aggregates; Impact of glycine and taurine to the PCB₄₃-*b*-PSB₁₅₈ aggregates (PDF)

AUTHOR INFORMATION

Corresponding Author

* Yuji Higaki – Department of Integrated Science and Technology, Faculty of Science and Technology, Oita University, 700 Dannoharu, Oita 870-1192, Japan; orcid.org/0000-0002-1032-4661; Email: y-higaki@oita-u.ac.jp

Author Contributions

The manuscript was written through the contributions of all authors, and all authors have approved the final version of the manuscript.

ACKNOWLEDGMENT

Y. Higaki gracefully acknowledges Izumi Science and Technology Foundation (Grant No. 2019-J-027), KOSÉ Cosmetology Research Foundation (Grant No. 694), for their financial support.

This work was performed under the Cooperative Research Program of “Network Joint Research Center for Materials and Devices”. This work was supported by Oita University President’s Strategic Discretionary Fund. The authors acknowledge Y. Saruwatari (Osaka Organic Chemical Industry Ltd.) for the kind donation of the carboxybetaine methacrylate monomer.

ABBREVIATIONS

PCB, poly(carboxybetaine); PSB, poly(sulfobetaine); DLS, dynamic light scattering; DP, degree of polymerization; CSL, inter-charge hydrocarbon spacer length

REFERENCES

1. Peer, D.; Karp, J. M.; Hong, S.; Farokhzad, O. C.; Margalit, R.; Langer, R. Nanocarriers as an Emerging Platform for Cancer Therapy. *Nat. Nanotechnol.* **2007**, *2*, 751-760.
2. Kataoka, K.; Harada, A.; Nagasaki, Y. Block Copolymer Micelles for Drug Delivery: Design, Characterization and Biological Significance. *Adv. Drug Delivery Rev.* **2001**, *47*, 113-131.
3. Discher, D. E.; Eisenberg, A., Polymer Vesicles. *Science* **2002**, *297*, 967-973.
4. Blazs, A.; Armes, S. P.; Ryan, A. J. Self-Assembled Block Copolymer Aggregates: From Micelles to Vesicles and their Biological Applications. *Macromol. Rapid Commun.* **2009**, *30*, 267-277.

5. Cabral, H.; Miyata, K.; Osada, K.; Kataoka, K. Block Copolymer Micelles in Nanomedicine Applications. *Chem. Rev.* **2018**, *118*, 6844-6892.
6. Peyret, A.; Zhao, H.; Lecommandoux, S. Preparation and Properties of Asymmetric Synthetic Membranes Based on Lipid and Polymer Self-Assembly. *Langmuir* **2018**, *34*, 3376-3385.
7. Chandler, D. Interfaces and the Driving Force of Hydrophobic Assembly. *Nature* **2005**, *437*, 640-647.
8. Schmidt, B. V. K. J. Double Hydrophilic Block Copolymer Self-Assembly in Aqueous Solution. *Macromol. Chem. Phys.* **2018**, *219*, 1700494.
9. Lira, R. B.; Willersinn, J.; Schmidt, B. V. K. J.; Dimova, R. Selective Partitioning of (Biomacro)molecules in the Crowded Environment of Double-Hydrophilic Block Copolymers. *Macromolecules* **2020**, *53*, 10179-10188.
10. Brosnan, S. M.; Schlaad, H.; Antonietti, M. Aqueous Self-Assembly of Purely Hydrophilic Block Copolymers into Giant Vesicles. *Angew. Chem., Int. Ed.* **2015**, *54*, 9715-9718.
11. Casse, O.; Shkilnyy, A.; Linders, J.; Mayer, C.; Häussinger, D.; Völkel, A.; Thünemann, A. F.; Dimova, R.; Cölfen, H.; Meier, W.; Schlaad, H.; Taubert, A. Solution Behavior of Double-Hydrophilic Block Copolymers in Dilute Aqueous Solution. *Macromolecules* **2012**, *45*, 4772-4777.
12. Nishimura, T.; Sumi, N.; Koda, Y.; Sasaki, Y.; Akiyoshi, K. Intrinsically Permeable Polymer Vesicles Based on Carbohydrate-Conjugated Poly(2-oxazoline)s Synthesized Using a Carbohydrate-Based Initiator System. *Polym. Chem.* **2019**, *10*, 691-697.

13. Nishimura, T.; Sasaki, Y.; Akiyoshi, K. Biotransporting Self-Assembled Nanofactories Using Polymer Vesicles with Molecular Permeability for Enzyme Prodrug Cancer Therapy. *Adv. Mater.* **2017**, *29*, 1702406.
14. Khimani, M.; Yusa, S.; Aswal, V. K.; Bahadur, P. Aggregation Behavior of Double Hydrophilic Block Copolymers in Aqueous Media. *J. Mol. Liq.* **2019**, *276*, 47-56.
15. Paschke, S.; Lienkamp, K. Polyzwitterions: From Surface Properties and Bioactivity Profiles to Biomedical Applications. *ACS Appl. Polym. Mater.* **2020**, *2*, 129-151.
16. Ishihara, K. Revolutionary Advances in 2-Methacryloyloxyethyl Phosphorylcholine Polymers as Biomaterials. *J. Biomed. Mater. Res., Part A* **2019**, *107*, 933-943.
17. Higaki, Y.; Kobayashi, M.; Takahara, A. Hydration State Variation of Polyzwitterion Brushes through Interplay with Ions. *Langmuir* **2020**, *36*, 9015-9024.
18. Mukai, M.; Cheng, C.-H.; Ma, W.; Chin, M.; Lin, C.-H.; Luo, S.-C.; Takahara, A. Synthesis of a Conductive Polymer Thin Film Having a Choline Phosphate Side Group and Its Bioadhesive Properties. *Chem. Commun.* **2020**, *56*, 2691-2694.
19. Schlenoff, J. B. Zwitteration: Coating Surfaces with Zwitterionic Functionality to Reduce Nonspecific Adsorption. *Langmuir* **2014**, *30*, 9625-9636.
20. Shao, Q.; Jiang, S. Molecular Understanding and Design of Zwitterionic Materials. *Adv. Mater.* **2014**, *27*, 15-26.

21. Georgiev, G. S.; Kamenska, E. B.; Vassileva, E. D.; Kamenova, I. P.; Georgieva, V. T.; Iliev, S. B.; Ivanov, I. A. Self-Assembly, Antipolyelectrolyte Effect, and Nonbiofouling Properties of Polyzwitterions. *Biomacromolecules* **2006**, *7*, 1329-1334.
22. Sakamaki, T.; Inutsuka, Y.; Igata, K.; Higaki, K.; Yamada, N. L.; Higaki, Y.; Takahara, A. Ion-Specific Hydration States of Zwitterionic Poly(sulfobetaine methacrylate) Brushes in Aqueous Solutions. *Langmuir* **2018**, *35*, 1583-1589.
23. Delgado, J. D.; Schlenoff, J. B. Static and Dynamic Solution Behavior of a Polyzwitterion Using a Hofmeister Salt Series. *Macromolecules* **2017**, *50*, 4454-4464.
24. Lim, J.; Matsuoka, H.; Yusa, S.; Saruwatari, Y. Temperature-Responsive Behavior of Double Hydrophilic Carboxy-Sulfobetaine Block Copolymers and Their Self-Assemblies in Water. *Langmuir* **2019**, *35*, 1571-1582.
25. Lim, J.; Matsuoka, H.; Saruwatari, Y. Effects of Halide Anions on the Solution Behavior of Double Hydrophilic Carboxy-Sulfobetaine Block Copolymers. *Langmuir* **2020**, *36*, 5165-5175.
26. Lim, J.; Matsuoka, H.; Saruwatari, Y. Effects of pH on the Stimuli-Responsive Characteristics of Double Betaine Hydrophilic Block Copolymer PGLBT-b-PSPE. *Langmuir* **2020**, *36*, 1727-1736.
27. Takahashi, M.; Shimizu, A.; Yusa, S.; Higaki, Y. Lyotropic Morphology Transition of Double Zwitterionic Diblock Copolymer Aqueous Solutions. *Macromol. Chem. Phys.* **2021**, *222*, 2000377.
28. Kratzer, D.; Barner, L.; Friedmann, C.; Bräse, S.; Lahann, J. A Synthetic Route to Sulfobetaine Methacrylates with Varying Charge Distance. *Eur. J. Org. Chem.* **2014**, 8064-8071.

29. Shao, Q.; Mi, L.; Han, X.; Bai, T.; Liu, S.; Li, Y.; Jiang, S. Differences in Cationic and Anionic Charge Densities Dictate Zwitterionic Associations and Stimuli Responses. *J. Phys. Chem. B* **2014**, *118*, 6956-6962.
30. Weers, J. G.; Rathman, J. F.; Axe, F. U.; Crichlow, C. A.; Foland, L. D.; Scheuing, D. R.; Wiersema, R. J.; Zielske, A. G. Effect of the Intramolecular Charge Separation Distance on the Solution Properties of Betaines and Sulfobetaines. *Langmuir* **1991**, *7*, 854-867.
31. Chevalier, Y.; Le Perchec, P. Intercharge Distance of Flexible Zwitterionic Molecules in Solution. *J. Phys. Chem.* **1990**, *94*, 1768-1774.

TOC graphic

